Explicit Hamiltonians Inducing Volume Law for Entanglement Entropy in Fermionic Lattices

Giacomo Gori,[1] Simone Paganelli,[2,3] Auditya Sharma,[3,4] Pasquale Sodano,[3,5,6] and Andrea Trombettoni[1,7]

[1]*CNR-IOM DEMOCRITOS Simulation Center, Via Bonomea 265, I-34136 Trieste, Italy*
[2]*Dipartimento di Scienze Fisiche e Chimiche, Università dell'Aquila, via Vetoio, I-67010 Coppito-L'Aquila, Italy*
[3]*International Institute of Physics, Universidade Federal do Rio Grande do Norte, 59078-400 Natal-RN, Brazil*
[4]*School of Chemistry, The Sackler Faculty of Exact Sciences, Tel Aviv University, Tel Aviv 69978, Israel*
[5]*Departemento de Fisíca Teorica e Experimental,*
Universidade Federal do Rio Grande do Norte, 59072-970 Natal-RN, Brazil
[6]*INFN, Sezione di Perugia, Via A. Pascoli, I-06123, Perugia, Italy*
[7]*SISSA and INFN, Sezione di Trieste, Via Bonomea 265, I-34136 Trieste, Italy*

We show how the area law for the entanglement entropy may be violated by free fermions on a lattice and look for conditions leading to the emergence of a volume law. We give an explicit construction of the states with maximal entanglement entropy based on the fact that, once a bipartition of the lattice in two complementary sets A and $\bar{A}$ is given, the states with maximal entanglement entropy (volume law) may be factored into Bell-pairs (BP) formed by two states with support on A and $\bar{A}$. We then exhibit, for translational invariant fermionic systems on a lattice, an Hamiltonian whose ground state is such to yield an exact volume law. As expected, the corresponding Fermi surface has a fractal topology. We also provide some examples of fermionic models for which the ground state may have an entanglement entropy S_A between the area and the volume law, building an explicit example of a one-dimensional free fermion model where $S_A(L) \propto L^\beta$ with β being intermediate between $\beta = 0$ (area law) and $\beta = 1$ (BP-state inducing volume law). For this model, the dispersion relation has a "zig-zag" structure leading to a fractal Fermi surface whose counting box dimension equals, for large lattices, β. Our analysis clearly relates the violation of the area law for the entanglement entropy of the ground state to the emergence of a non-trivial topology of the Fermi surface.

I. INTRODUCTION

The study of entanglement in quantum systems has been a major field of research in the last two decades. Motivations for this are various and important since entanglement provides not only a characterization of quantum states [1–3] and a pathway on how to simulate them with numerical tools such as DMRG [4] and tensor network states [5], but it helps also to characterize quantum phase transitions [6–8] and to detect novel quantum phases, including topological phases. Non-trivial, explicit examples of the use of entanglement-related quantities, such as entanglement spectrum and negativity, range from quantum Hall states [9–11] to Bose-Hubbard [12] and Kondo models [13, 14]. In addition the study of entanglement allows to characterize the computational power of quantum phases [15–18].

A key quantity entering the characterization of entanglement is provided by the Entanglement Entropy (EE). For its definition one takes a partition of a given system in two subsystems A and $\bar{A}$ (the complement of A), determines the reduced density matrix of a subsystem (say, of A) ρ_A by tracing out the degrees of freedom in $\bar{A}$ and then computes its entropy: $S_A = -Tr_A(\rho_A \ln \rho_A)$ [2]. The celebrated *area law* [19, 20] for the EE refers to the fact that typically the EE grows as the boundary of the subsystem A: i.e., for a system in d dimensions and a subsystem of size L having volume $\sim L^d$ and area $\sim L^{d-1}$, $S \sim L^{d-1}$ according of the area law [19, 21, 22].

The study of EE in various models has been recently a subject of intense research: EE can be explicitly computed in non-interacting systems of bosons and fermions [23–28], including trapped fermions [29], in integrable [30–32] and 1D critical models [33–36], and in spin chains with long-range interactions [37]. An important result is that, for gapless $1d$ integrable systems, the EE grows as $\ln L$, and that the prefactor is proportional to the central charge of the model. The next-leading term of the EE has been studied as well: e.g., for $2d$ systems the size-independent constant entering S is the so-called topological EE [38, 39]. Furthermore, the EE of a subsystem made of two disjoint intervals has been also intensively studied [40–42]: for these issues we refer the interested readers to [43].

A first possible deviation from the area law is provided by logarithmic corrections: as shown in [25, 26, 44, 45], for (critical) fermionic systems of dimension d, the EE of a subsystem of size L typically grows as $S_A \sim L^{d-1} \ln L$ (this result does not hold for bosonic systems [24]). An explicit expression for the prefactor entering S_A in dimension larger than 1 may be given using the Widom conjecture [26], and is found in remarkable agreement with numerical results [46, 47]. Entropy bounds for reduced density matrices of fermionic states were given in [48, 49]; the role of disorder was also investigated [50], and it was shown that the momentum space entanglement spectrum reveals the location of delocalized states in the energy spectrum [51] and that the entanglement structure depends only on the probability distribution of the length of the effective bonds [52]. Furthermore, allowing for long-range interactions leads to a

logarithmically diverging EE in gapped noncritical models [53], in spin chains [54] and Bose-Einstein condensates [55]. Non-local exponentially decaying couplings were considered in [56]: at intermediate distances a volume law is observed, but as soon as L becomes of the order of the length scale of the decay of the couplings the area law is recovered.

Pertinent inhomogeneous couplings in simple spin chain Hamiltonians with only nearest-neighbor interactions have been shown to induce a volume law in absence of translational invariance [57]. A violation of the area law for bosonic systems with Bose surfaces was analyzed in [58]. Fermi liquids are expected to obey the area law while non-Fermi liquids in $2d$, although have been shown to satisfy the area law, are at the border between area law and non-area law EE [59, 60]. A construction of a translation invariant fermionic state violating the area law was explicitly given in [61], when the Fermi surface is a Cantor-like set. Non-logarthmic deviations from the area law were also observed in [62], where two different kinds of disordered fermionic chains were considered. An analysis of EE in spin chains having long-range interactions and a fractal Fermi surface for the associated Jordan-Wigner fermions has been presented in [63, 64]: in particular in [64] it was shown that EE for all translational-invariant pure states is at least logarithmic and there is an arbitrary fast sublinear entropy growth.

States supporting an area law for the EE are not maximally entangled and yet maximally entangled states have been deeply studied both for their intrinsic interest and in connection to quantum information protocols: maximally multiqubit entangled states up to eight qubits in qubit registers were reported in [65–69], while applications of absolutely maximally entangled states (i.e., multipartite quantum states maximally entangled with respect to any possible bipartition) to a variety of quantum information protocols, including quantum secret sharing schemes [70, 71] and open-destination teleportation protocols [72].

In this paper we show that a volume law for the EE of the ground state may emerge in fermionic lattices: to avoid ambiguities, we say that the a violation of the area law is obtained if, apart from logarithmic corrections, the EE scales as $S_A \sim L^\beta$, with $\beta > d - 1$. In particular, for $1d$ chains, a violation of the area law corresponds to $\beta > 0$ and for $\beta = 1$ we have the volume law. To set the notation, we write the Hamiltonian of (spinless) free fermions hopping on a generic lattice as

$$H = -\sum_{I,J} c_I^\dagger t_{IJ} c_J. \tag{1}$$

The lattice has N_S sites and its connectivity is characterized by the hopping matrix t_{IJ} with $t_{IJ} = t_{JI}^*$; of course c_I and $c_I^\dagger$ are the annihilation and creation fermionic operators on the site I. The number of fermions is N_T, and the filling is then $f = N_T/N_S$ ($0 \le f \le 1$). The sites of the lattice are denoted by capital letters $I, J = 1, \cdots, N_S$ while the sites of a generic subsystem having L sites are denoted by (small) letters $i, j = 1, \cdots, L$. If the system is in the pure state $|\Psi\rangle$, the EE of the subsystem A is given by

$$S_A = -\sum_{\gamma=1}^{L} \left[(1 - C_\gamma) \ln (1 - C_\gamma) + C_\gamma \ln C_\gamma \right], \tag{2}$$

where C_γ is one of the L eigenvalues of the correlation matrix

$$C_{ij} = \langle \Psi | c_i^\dagger c_j | \Psi \rangle. \tag{3}$$

In Appendix A, following [27], we provide an explicit expression of the correlation matrix C_{ij} if $|\Psi\rangle$ is the ground-state of the Hamiltonian (1), which is the situation we are going to mostly consider.

From Eq. (2), one easily sees that for the EE to satisfy the volume law, one may construct a state for which each C_γ is equal to $1/2$ since for this state $S_A = -L \ln \frac{1}{2}$. In the following, we shall provide a method for the construction of such states and give some examples of Hamiltonians supporting as a ground state a state with maximal EE. We get the remarkable result that, associated with these states, Fermi surfaces with nontrivial topology naturally emerge.

At first sight one might think that a volume law could emerge only as a result of introducing a long-range hopping matrix t_{IJ} in the Hamiltonian (1). Our analyses shows that this is not the case since, at least for translational invariant systems, it is rather the topology of the Fermi surface which really matters, as also pointed out in previous analysis [44]. Indeed we demonstrate that, give a partition of the single-particle Hilbert space to orthogonal subspaces $\mathcal{A}$ and $\bar{\mathcal{A}}$ the state yielding maximal EE may be factorized into Bell-pairs formed by two states belonging to $\mathcal{A}$ and $\bar{\mathcal{A}}$. We call such state Bell-paired state (BP-state). As we shall see explicitly, for translational-invariant Hamiltonians, the BP-states are highly nonlocal in the space and the Fermi surfaces have nontrivial topology.

The paper is organized as follows: in Sec. II we analyze a free fermion model with hoppings decaying as a power law with exponent α. We find that the EE obeys to the area law for each finite and positive α, even tough, for $\alpha < 1$ the energy is not extensive [73]; only for $\alpha = 0$, i.e. for the fully connected lattice, one has a volume law for the EE since

$S_A \propto L$. Unfortunately, the fully connected lattice is pathological in many respects, since the Fermi level is infinitely degenerate and the number of sites of a given subsystem A is at the same time its volume and its surface (defining on a graph the volume of a subgraph as the number of vertices on it and the surface as the number of vertices on it linked to vertices outside the subgraph itself [74, 75]).

In Sec. III we explicitly construct, for any given lattice and arbitrary filling f, the general form of the states rendering the EE and all the Rényi entropies maximal. This construction allows for to have an explicit momentum representation of the state with maximal entanglement entropy. In Sec. IV we provide explicit examples of Hamiltonians supporting a BP-state as the ground state and analyze the topology of their Fermi surface. Sec. V is devoted to our concluding remarks, and in the appendices A B C we provide the reader with technical details about the models described in the main text. In Appendix D we analyze the violation of the area law of the ground state for a free fermionic model which is not translational invariant.

II. FREE FERMIONS WITH NON-LOCAL POWER-LAW HOPPINGS

In this Section we focus our attention on a translationally invariant one-dimensional chain, with non-local hopping matrix $t_{I,J}$ given by

$$t_{I,J} = \begin{cases} 0 & I = J, \\ \frac{t}{|I-J|_p^\alpha} & I \neq J, \end{cases} \tag{4}$$

where the distance $|\cdot|_p$, due to periodic boundary conditions, is defined as

$$|I - J|_p = \min(|I - J|, N_S - |I - J|). \tag{5}$$

The hopping matrix, being translationally invariant, is readily diagonalized: its eigenstates are given by plane waves and, in the thermodynamic limit, the energy spectrum is

$$\varepsilon_k = -2t\ell_\alpha(k), \tag{6}$$

where $k = 2\pi n_k/N_S$ belongs to the first Brillouin zone ($n_k = -N_S/2, \cdots, N_S/2 - 1$ for even N_S) and

$$\ell_\alpha(k) = \sum_{m=1}^\infty \frac{\cos(mk)}{m^\alpha}, \tag{7}$$

(with $\alpha > 1$). As usual, even if for $\alpha \leq 1$ the ground-state energy in the thermodynamic limit diverges, one can make the energy extensive by the so-called Kac rescaling [73].

The function ε_k is plotted for two values of $\alpha > 1$ in Fig.1. One sees that the spectra are monotonic for $k > 0$ and $k < 0$, and, thus, the filling of the momentum eigenstates leading to the occupation of the Fermi sea is the same for each value of $\alpha > 1$. The same result holds also for $0 < \alpha \leq 1$ for any finite number of sites (Appendix B). As a consequence, the EE does not change since the correlation matrix (3) depends only on the ground state (and not on the spectrum); in the thermodynamic limit, $S_A \sim \ln L$ for each $\alpha > 0$ for any filling f, just as it happens if the hopping t_{IJ} was short range [25]. A similar analysis, yielding the same results, may be carried out also for $t < 0$ and $t = (-1)^{i-j}|t|$.

Things change for $\alpha = 0$. Here, it is easy to verify that the single-particle energy spectrum is made of a non-degenerate ground-state and of an $(N_S - 1)$-fold degenerate excited state, implying that the many-body ground-state is highly degenerate. In addition, the Fermi surface passes from a two-point set (as it happens for $\alpha > 0$) to a continuous set. In Appendix C we show that, for $N_S \gg 1$,

$$S_A = -L\left[(1 - f)\ln(1 - f) + f\ln(f)\right]; \tag{8}$$

in particular, $S_A = L \ln 2$ for $f = 1/2$. This corresponds to an equal *a priori* probability of occupation of all degenerate states by the available particles.

The fully connected hopping model does not have a specific dimensionality d: however, if we think it as the $\alpha \to 0$ limit of a d-dimensional long-range hopping model and A is a cubic subsystem with size $\mathcal{L}$, then the number L of sites of A is given by $L \sim \mathcal{L}^d$.

It appears as we already obtained a volume law for the EE. Unfortunately, for the fully connected hopping model, the number of sites L of the subsystem A is at the same time the volume and the surface of A in the sense that all the L sites of A are linked with the other sites of the rest of the system $\bar{A}$. In addition the mutual information
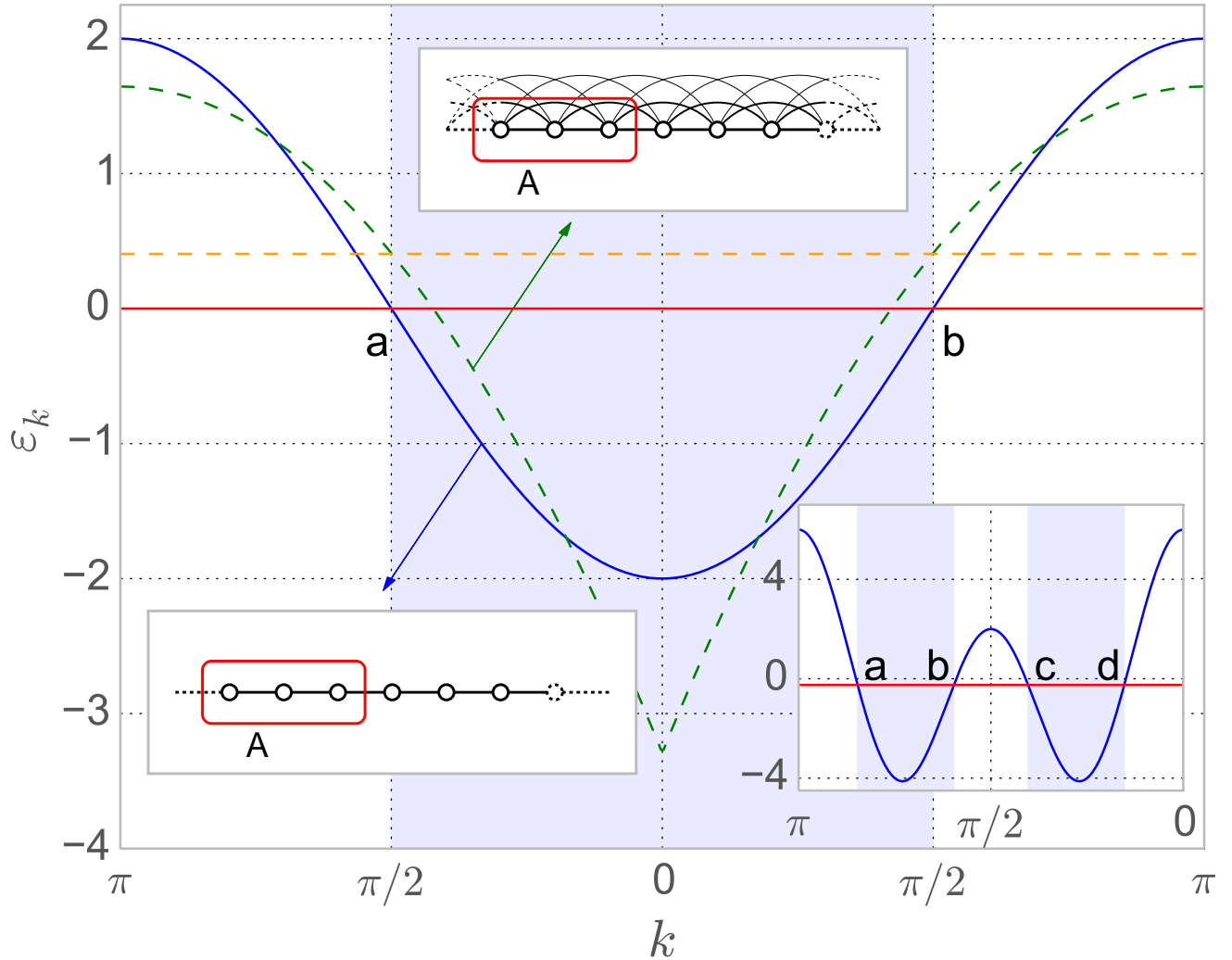
FIG. 1: Energy spectra ε_k (in units of t) of a model with nearest-neighbor hopping corresponding to $\alpha \to \infty$ (solid line) and non-local hoppings with $\alpha = 2$ (dashed line) in the thermodynamic limit. The horizontal lines represent the Fermi energy at half-filling for both models. The regions of k-space comprised within the points a and b are the occupied wave vectors, indicated in the whole diagram with a (pale blue) shading. In the white (top and bottom left) the hopping structures of both models are represented - in the bottom right inset the energy spectrum for a next-nearest-neighbor model having four Fermi points (denoted by a, b, c and d) is plotted ($t_1 = t$, $t_2 = -2t$).

between A and $\bar{A}$ is vanishing for $N_S \gg 1$ and, thus, the emergence of a volume law corresponds here to nothing but the transition to a classical state.

The analysis carried out in this Section shows that, for translational invariant systems, long-range hoppings alone are not enough to guarantee the emergence of the volume law for the EE and it appears that the structure of the Fermi surface is bound to play a key role in the behavior of the EE. In particular, for a translational invariant chain and a quadratic Hamiltonian of the form (1), all the models having Fermi wave vectors k_a and k_b at the points a, b of Fig.1 have the same correlation matrix, which, in the continuum limit, reads

$$C_{ij} = \int\limits_{k_a}^{k_b} \frac{dk}{2\pi} e^{ik(i-j)}, \tag{9}$$

leading to the same EE (we remind that our Hamiltonian (1) does not include any "superconducting" $c_I^\dagger c_J^\dagger, c_I c_J$ terms, that would change the correlation matrix (9)). If $-k_a = k_b \equiv k_F$ then the well known result $C_{ij} = \sin[k_F(i-j)]/[\pi(i-j)]$ of the nearest-neighbor free fermionic chain is recovered [23].
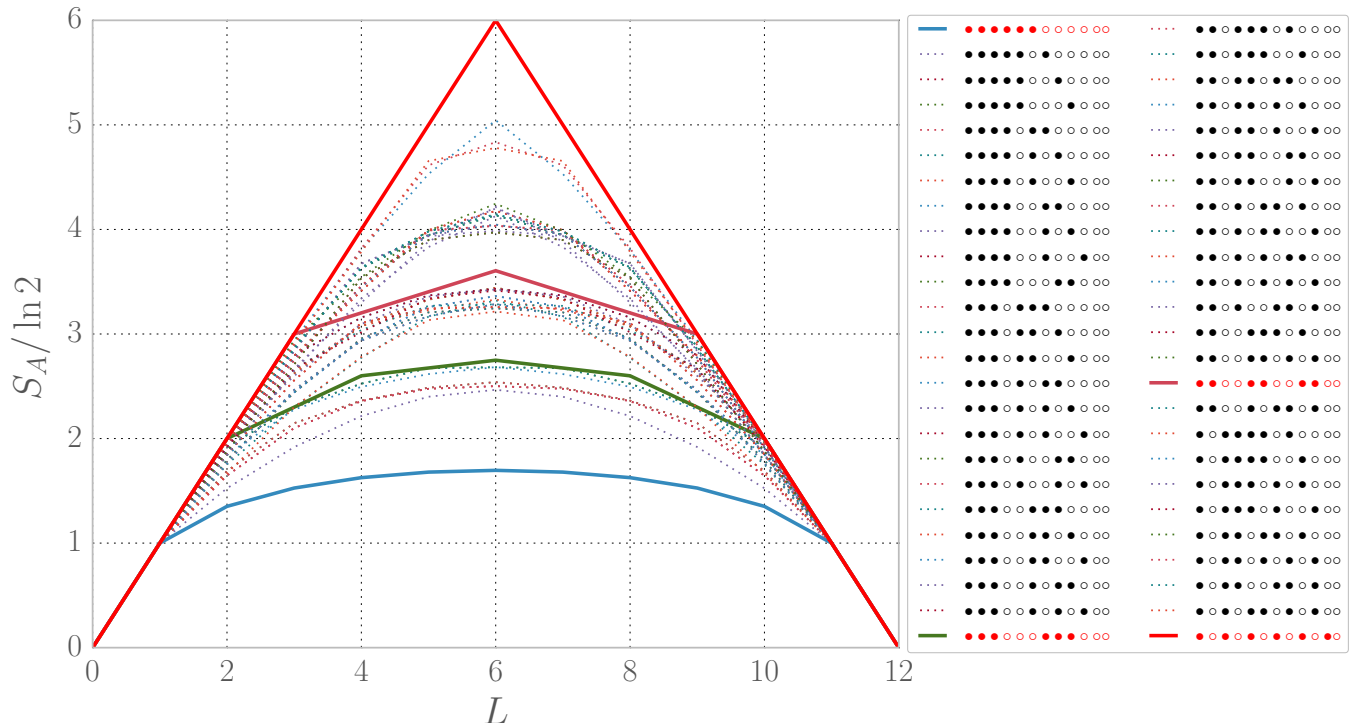
FIG. 2: EE in terms of the subsystem length L for all the combinatorially distinct Fermi surfaces for a system of $N_S = 12$ sites at half-filling. In the right legend a filled (empty) dot denote a filled (unoccupied) momentum eigenstate. The states are ordered with respect to increasing k (modulo 2π). The states having a periodic structure in k-space are highlighted in the legend with a color red and are plotted in the left figure with thick continuous lines: the lower thick blue line refers to momenta occupied up to k_F (resulting in logarithmic EE), the upper thick red line refers to the state with alternating filled momenta (having linear EE), the central thick scarlet and green lines to the states having sequence of two (three) filled momenta and two (three) holes.

To better clarify the role played by the Fermi surface let us consider the energy spectrum represented in the bottom right inset of Fig.1 having 4 Fermi wave vectors k_a, k_b, k_c, k_d at the points a, b, c, d: the same argument leading to (9) yields

$$C_{ij} = \int\limits_{k_a}^{k_d} \frac{dk}{2\pi} e^{ik(i-j)} - \int\limits_{k_b}^{k_c} \frac{dk}{2\pi} e^{ik(i-j)}. \tag{10}$$

(this formula can be easily generalized to Fermi surfaces with wave vectors $k_1, \cdots, k_{2m}$). As a result, the EE depends only on k_a, k_b, k_c, k_d and not on other details of the energy spectrum.

III. STATES WITH MAXIMAL ENTANGLEMENT ENTROPY

In order to elucidate the role played by the Fermi surface for constructing a maximal entangled state in a translationally invariant free fermionic lattice, it is instructive to look at *all* the possible Fermi surfaces arising in 1-dimensional systems of small size N_S. This task is simplified if one notices that circular shifts ($k \to k + 2n_k\pi/N_S, n_k \in \mathbb{Z}$) and reflections ($k \to -k$) of the Fermi surface do not alter the EE. As a result, the number of Fermi surfaces yielding different values of the EE is much reduced; from combinatorics this number is obtained by counting all the distinct reversible bracelets [76, 77]. The result is shown in Fig.2 for a system with $N_S = 12$ sites at half-filling. As one can see, the Fermi surfaces exhibiting the maximal EE are realized with an alternating filling of the wave vectors periodic in k-space with period 2, while Fermi surfaces exhibiting higher periodicity in k-space, have a piecewise linear behavior. The minimal EE for a system of 12 sites at half filling is achieved with a Fermi surface made up of two points, i.e. made occupying 6 states with adjacent wave vectors. Similar findings are obtained for different system sizes and fillings. This procedure allows to explicitly construct a state of maximal EE for small fermionic systems through a pertinent

filling of the Fermi sea. In addition, once the sistem size and the filling are given, it selects the Fermi surface for which a volume law emerges.

In the following, we shall generalize the above result to systems of finite, but arbitrarily large, size N_S.

As shown in Sec. I, the EE between A and $\bar{A}$ for a non-interacting fermionic system in its ground-state is determined by the correlation matrix (3), which may be usefully rewritten as

$$C_{i,j} = \sum_{b \in B} \langle i|b\rangle\langle b|j\rangle \quad (i,j \in A),\tag{11}$$

where B labels the set of single particle states entering in (11).

To compute the EE one needs to find the eigenvalues C_γ of the matrix $C_{i,j}$. In the following, we denote with $\mathcal{A}$ and $\mathcal{B}$ two nonorthogonal subspaces of the single-particle state space $\mathcal{H}$ such that $\mathcal{A} = \mathrm{span}\{|i\rangle, i \in A\}$ and $\mathcal{B} = \mathrm{span}\{|b\rangle, b \in B\}$. We then define $P_\mathcal{A}$ and $P_\mathcal{B}$ as the projection operators over the subspaces $\mathcal{A}$ and $\mathcal{B}$, respectively. Upon introducing the operator

$$\Gamma = P_\mathcal{A}P_\mathcal{B}P_\mathcal{A},\tag{12}$$

one has that

$$C_{i,j} = \langle i|\Gamma|j\rangle,\tag{13}$$

with $i,j \in A$. As a result the EE can be written as

$$S_A = S_{\mathcal{A},\mathcal{B}} = -\mathrm{Tr}\left[\Gamma \ln \Gamma + (1-\Gamma)\ln(1-\Gamma)\right].\tag{14}$$

With the notation used in (14), the symmetries of S_A are made manifest since $S_{\mathcal{A},\mathcal{B}} = S_{\mathcal{A},\bar{\mathcal{B}}}$ and $S_{\mathcal{A},\mathcal{B}} = S_{\bar{\mathcal{A}},\mathcal{B}}$ (where $\bar{\mathcal{B}}$ is the orthogonal complement of $\mathcal{B}$).

In the following we shall determine, for a given $\mathcal{A}$, the vector space $\mathcal{B}$ for which the EE is maximal. As we shall see, for translational invariant free fermionic lattices, this amounts to determine the topology of the Fermi surface maximizing the EE.

The EE is strictly upper bounded by the dimension of the smallest space between $\mathcal{A}$ and $\bar{\mathcal{A}}$ times $\ln 2$, since in Eq. (14) natural logarithms have been used. Of course, $\dim \mathcal{A} = |A|$ and $\dim \bar{\mathcal{A}} = |\bar{A}|$, where $|A| = L$ ($|\bar{A}| = N_S - L$) is the cardinality of the set A ($\bar{A}$). As a result

$$S_{\mathcal{A},\mathcal{B}} \le S_{\max} = \ln 2 \cdot \min(|A|,|\bar{A}|).\tag{15}$$

We shall now explicitly construct the states satisfying this upper bound. We observe that, in the construction of maximal EE states, we do not need to fix the dimension of $\mathcal{B}$, i.e. the number of fermions ($\dim \mathcal{B} = N_T$). Indeed, if $|A| = L \le \frac{N_S}{2}$, we shall show that the maximal EE $S_A = L\ln 2$ is obtained when the filling fraction f is such that $\frac{L}{N_s} \le f \le 1 - \frac{L}{N_s}$. It follows that, for fixed N_S, the maximal EE is obtained for $L = \frac{N_S}{2}$ and $f = \frac{1}{2}$.

For simplicity we set $|A| \le |\bar{A}|$, the case $|A| \le |\bar{A}|$ can be similarly worked out by exchanging A and $\bar{A}$. Since the number of nonzero eigenvalues of the hermitean operator Γ is smaller or equal than $|A|$ and the maximum contribution of each of these eigenvalues to the total EE is $\ln 2$, we conclude that, in order to obtain the maximum EE, Γ should have $|A|$ eigenvectors $|\alpha_i\rangle$, $i = 1,\ldots,|A|$ with eigenvalue $1/2$. Namely, one should have

$$\Gamma|\alpha_i\rangle = (1/2)|\alpha_i\rangle.\tag{16}$$

From the definition of Γ, one easily sees that, in order to have a maximum EE state, $|B|$ should be at least equal to $|A|$. As a consequence, if the subspace $\mathcal{B}$ is spanned by the orthonormal vectors $|\beta_1\rangle, |\beta_2\rangle, \ldots |\beta_{|B|}\rangle$, (so that $P_\mathcal{B} = \sum_{i=1}^{|B|} |\beta_i\rangle\langle\beta_i|$), without loss of generality, one may choose the first $|A|$ vectors $|\beta_i\rangle, \ldots, |\beta_{|A|}\rangle$ to have a nonzero projection on $\mathcal{A}$. One has then that

$$|\beta_1\rangle = \gamma_1|\alpha_1\rangle + \bar{\gamma}_1|\bar{\alpha}_1\rangle, |\beta_2\rangle = \gamma_2|\alpha_2\rangle + \bar{\gamma}_2|\bar{\alpha}_2\rangle, \ldots, |\beta_{|A|}\rangle = \gamma_{|A|}|\alpha_{|A|}\rangle + \bar{\gamma}_{|A|}|\bar{\alpha}_{|A|}\rangle.\tag{17}$$

where the complex coefficients $\gamma_i, \bar{\gamma}_i$ are yet to be determined, the $|\alpha_1\rangle, |\alpha_2\rangle, \ldots, |\alpha_{|A|}\rangle$ are an orthonormal basis for $\mathcal{A}$ and the $|\bar{\alpha}_1\rangle, |\bar{\alpha}_2\rangle, \ldots, |\bar{\alpha}_{|A|}\rangle$ are orthonormal vectors in $\bar{\mathcal{A}}$. Of course, additional vectors will not give rise to nonzero eigenvalues of Γ thus we can limit ourselves to $|B| = |A|$ i.e. we are determining $\mathcal{B}$ up to vectors orthogonal to $\mathcal{A}$
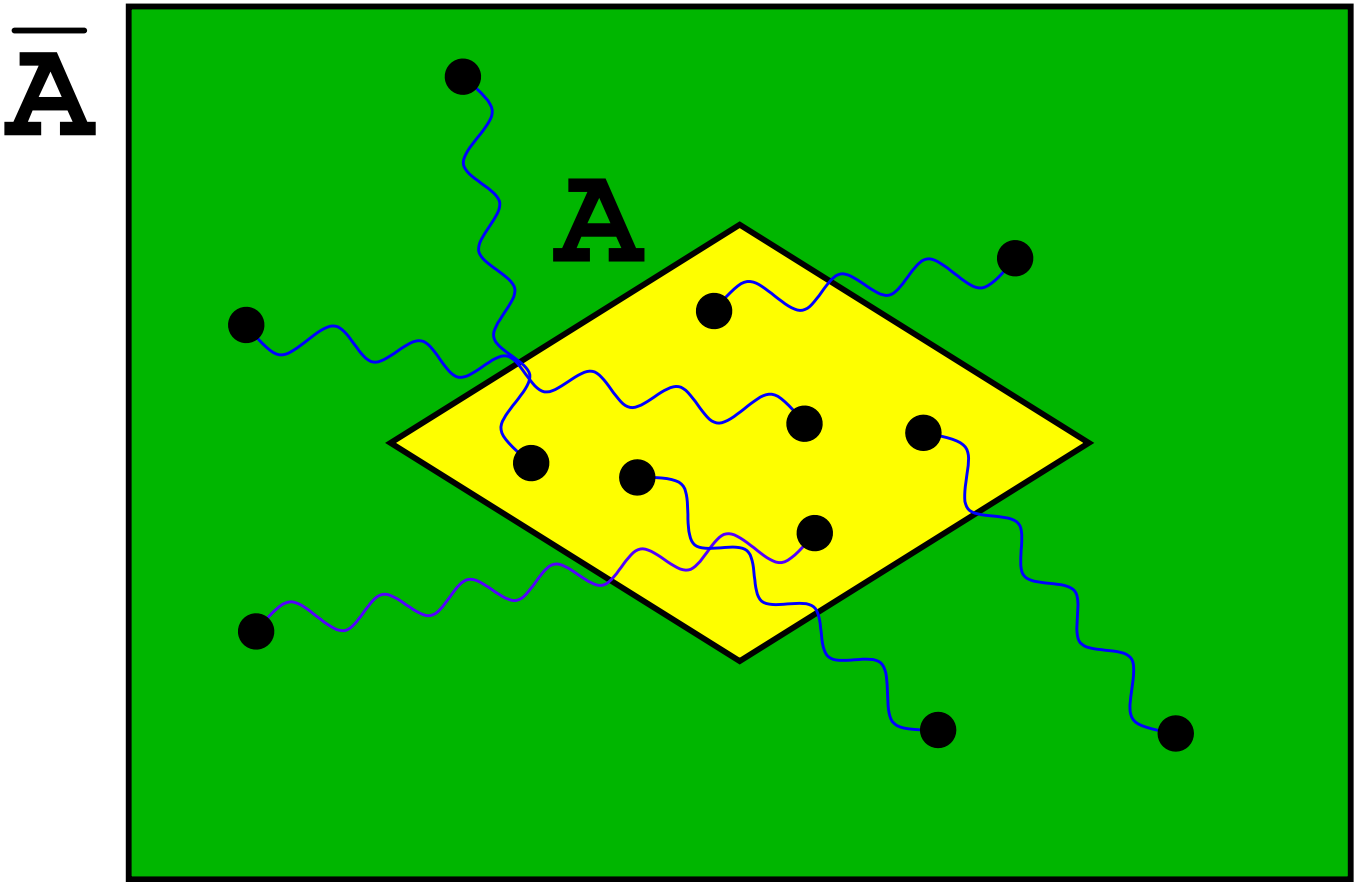
FIG. 3: Pictorial representation of a BP-state.

[78]. The above decomposition indeed is similar to the one obtained in [49] where it was used in order to obtain *lower bounds* for the entanglement entropy in a fermionic systems.

By requiring that (16) is satisfied, one gets that $|\gamma_i|^2 = |\bar{\gamma}_i|^2 = 1/2$ ($i = 1, \cdots, |A|$). Without loss of generality one may choose $\gamma_i = \bar{\gamma}_i = 1/\sqrt{2}$, thus $\mathcal{B}$ is spanned by:

$$|\beta_1\rangle = \frac{1}{\sqrt{2}}(|\alpha_1\rangle + |\bar{\alpha}_1\rangle), |\beta_2\rangle = \frac{1}{\sqrt{2}}(|\alpha_2\rangle + |\bar{\alpha}_2\rangle), \ldots, |\beta_{|A|}\rangle = \frac{1}{\sqrt{2}}(|\alpha_{|A|}\rangle + |\bar{\alpha}_{|A|}\rangle). \tag{18}$$

This determines the form of the maximal EE state, and explicitly shows that, given $\mathcal{A}$, the space $\mathcal{B}$ maximizing the EE is made out of L Bell-paired states among A and $\bar{A}$. In the following we shall refer to these states as BP-states. A BP-state is pictorially represented in Fig. 3.

It should be stressed that

- in our construction the nature of the set $\mathcal{B}$ is left unspecified, the only natural requirement being that it is a set of allowed single particle states. Only for translational invariant systems the set B may coincide with the set of single particle momentum states;

- the set A does not need to be simply connected: in particular, if A it is not simply connected the BP-states provided by the indicated construction are not localized around the sites;

- if, instead, the set B is fixed, our construction allows to determine the set A yielding the state with maximal EE;

- if one wishes to find maximal EE states as the size of A is enlarged, the problem to be considered is the following: given a sequence of sets $\{A_i\}, i = 1, \ldots, N_S$ (with $A_i \subset A_j$ if $i < j$) to which corresponds a set of linear spaces $\{\mathcal{A}_i\}$ one should determine a subspace $\mathcal{B}$ for which the EE is maximal for every i. For this purpose it is enough to construct the basis (18) when $|A|_i = N_S/2$ for N_S even or $|A|_i = (N_S - 1)/2$ for N_S odd: in other words the maximal EE states are obtained at half-filling and have $S = L \ln 2$ for $L \leq N_S/2$ as plotted in Fig.2, red line;

- the BP-state also maximizes the Rényi entropy of order ν since, for $L \leq N_S$,

$$S_\nu = \frac{1}{1-\nu} \ln \sum_{\gamma=1}^{L} \left[(C_\gamma)^\nu + (1-C_\gamma)^\nu \right].$$ (19)

As one can easily verify that the Rényi entropy of order ν is bounded from above by $S_{\max}$ and attains a maximum when all the C_γ are equal to $1/2$: therefore, for a BP-state, all the Rényi entropies are maximal and equal to the maximum value of the EE $S_{max} = L \ln 2$.

Let us consider now a spatial partition in which A is a simply connected subsystem of the lattice: then the states in A sharing the Bell-pairs with $\bar{A}$ are localized around sites. One then expects that, plotting $C_{i,j}$ $(i,j \in A)$ for a maximal EE state, yield $C_{i,j} = 1/2\delta_{i,j}$. A useful quantity to visualize the correlations emerging between $\mathcal{A}$ and $\bar{\mathcal{A}}$ is the correlator $\mathcal{C}_{I,J} = \langle c_I^\dagger c_J + c_J^\dagger c_I \rangle$ which equals $C_{I,J} + C_{J,I}^*$ if I and J belong to A. We plot $|\mathcal{C}_{I,J}|$ for various states in Fig.4, where the correlation matrix $\mathcal{C}_{i,j}$ of A is the one on the top left part of $\mathcal{C}_{I,J}$.

The translationally invariant states obtained by occupying contiguous momentum eigenvectors up to the Fermi wave vector are characterized by an alternating pattern of zero and nonzero diagonals as we move away from the main diagonal (which is by construction equal to one), as shown in panel (a) of Fig.4. The maximal EE state for translational invariant states is plotted in panel (b) and it is made out of four identity submatrices. It should be noticed that the BP- state is made out of Bell pairs connecting sites at distance $N_S/2$.

The panel (c) instead refers to a state where the occupation in k-space alternates in the momentum space sequences of two filled states and two holes (in Fig.2 its EE is represented with the continuous scarlet line and it does not have maximal EE). Finally panel (d) shows the general structure of a BP-state having maximal EE obtained coupling $N_S/2$ randomly chosen orthogonal states $\{|\alpha_i\rangle\}$ in subspace $\mathcal{A}$ and $N_S/2$ randomly chosen orthogonal states $\{\bar{\alpha}_i\}$ in subspace $\bar{\mathcal{A}}$.

Notice that, by a change of basis, the maximal EE state plotted in panel (d) may be represented as in panel (b). One concludes that the condition that the top left matrix of the matrix $\mathcal{C}_{I,J}$ is diagonal is sufficient to have a maximal EE state.

IV. MODELS VIOLATING THE AREA LAW: EXPLICIT HAMILTONIANS AND THEIR FERMI SURFACES

We shall exhibit here a few one-dimensional models and supporting ground-states leading to a violation of the area law, and we shall look at the nontrivial topology of the Fermi surface.

For this purpose we firstly notice that, for a translationally invariant chain and for A a simply connected domain such that $|A| = N_S/2$, the maximum EE state may be obtained by occupying the even (or odd) momentum eigenvectors. Indeed, a basis of $\mathcal{A}$ is given by vectors $|\alpha_k\rangle$ such that

$$\langle J|\alpha_k\rangle = \begin{cases} \frac{1}{\sqrt{N_S/2}} e^{ikJ} & \text{for } J \leq N_S/2 \\ 0 & \text{for } J > N_S/2, \end{cases}$$ (20)

while a basis of $\bar{\mathcal{A}}$ is given by vectors $|\bar{\alpha}_k\rangle$ such that

$$\langle J|\bar{\alpha}_k\rangle = \begin{cases} 0 & \text{for } J \leq N_S/2 \\ \pm\frac{1}{\sqrt{N_S/2}} e^{ikJ} & \text{for } J > N_S/2. \end{cases}$$ (21)

In Eqs. (21) and (20) $k = 4\pi n_k/N_S$ with $n_k = -N_S/4, \cdots, N_S/4 - 1$ and the $\pm$ accounts for the filling of the even and odd frequencies respectively. One sees that the subspace spanned by (18) is the state with only the even (odd) frequencies occupied. This is a BP-state maximizing the EE.

Notice that, if we choose a state with an alternating sequence of two filled momenta and two holes, then the EE is linear up to $L = N_S/4$: for $N_S = 12$ this corresponds to the EE thick scarlet line of Fig.(4), i.e., the 15th state from top in the right part of the legend of the same figure. Similarly, for the state with an alternating sequence of three filled momenta and three holes, the EE is linear up to $L = N_S/6$: for $N_S = 12$ this corresponds to the EE thick green line of Fig.(4), i.e., the bottom state in the left part of the legend. For general N_S at half-filling, a state having a sequence of n filled momenta and n holes (with N_S multiple of $2n$) will have linear EE up to $L = N_S/2n$.

A simple Hamiltonian supporting a BP-state as a ground state, thus yielding the volume law for the EE, has the form (1) with a hopping matrix $t_{I,J}$ given by (with even N_S)

$$t_{I,J} = \begin{cases} -t & for \ |I-J|_p = \frac{N_S}{2} \\ 0 & otherwise, \end{cases}$$ (22)
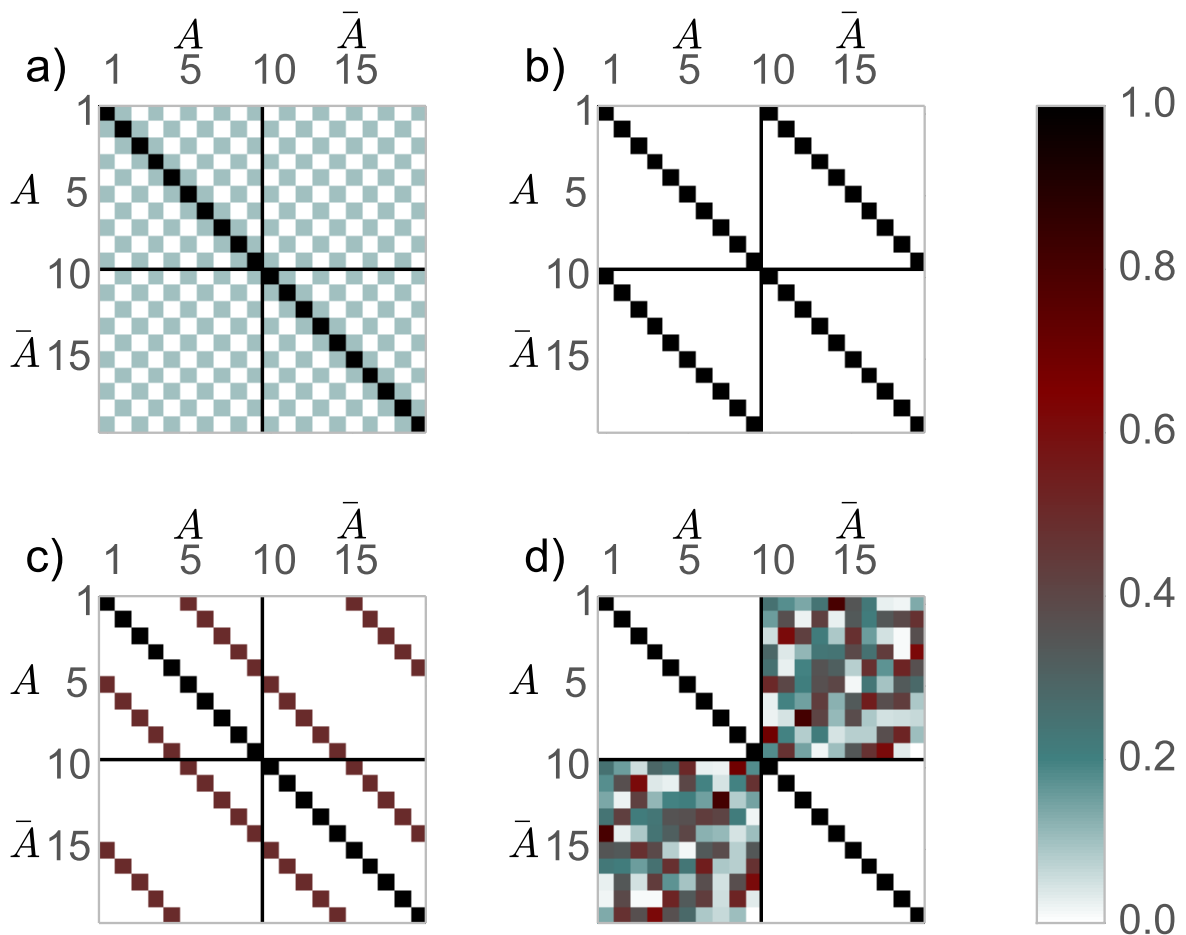
FIG. 4: Absolute value of the matrix elements of the correlator $\mathcal{C}_{I,J}$ for four different kind of entangled states at half-filling in a system with $N_S = 20$. The four matrices a, b, c, and d refer to a state with ferromagnetic hopping, zigzag state, a state with two filled states and two holes alternatively and a generic BP-state respectively.

with $t > 0$ and periodic boundary conditions. Notice that, in (22), only hoppings between sites distant $N_S/2$ are allowed. At half-filling, the ground-state is constructed by occupying only the states with n_k even (occupation of the states with n_k odd is obtained for $t < 0$). As a result, the Fermi surface has a fractal topology and its counting box dimension d_{box} [79] equals to 1. This example provides an explicit and simple setting where the emergence of the volume law is associated to a non-trivial topology of the Fermi surface: this sheds light on the results of previous investigations [25, 61]. Slight modifications of the hoppings (22) can be built to have states having sequences of n filled momenta and n holes.

Fractal Fermi surfaces may be realized as pertinent limits of other model Hamiltonians. In the following we analyze two specific models where this happens.

A. Model A

A possible way to obtain a fractal Fermi surface is to consider the effect of a phase in a model with long-range hoppings:

$$t_{I,J} = \frac{t \cdot e^{i\phi d_{I,J}}}{|I - J|_p^\alpha}, \tag{23}$$

where $\phi = \frac{2\pi}{N_S}\Phi$, being Φ a constant and $d_{I,J}$ the oriented distance between the sites I and J, whose definition is given in (B2).

The spectrum of the ensuing hopping Hamiltonian is analyzed in Appendix B. For odd N_S the eigenvalues are given by $\varepsilon_k = -2t\ell_\alpha(k; N_S)$ where

$$\ell_\alpha(k; N_S) = \sum_{m=1}^{(N_S+1)/2} \frac{\cos\left[m\left(k+\phi\right)\right]}{m^\alpha}; \tag{24}$$

as usual, $k = 2\pi n_k/N_S$ with $n_k = 0, \cdots, N_S - 1$. A similar formula is obtained for even N_S.

For $\phi = 0$, the spectrum is always monotonous in the interval $k \in [0, \pi]$, while for $\phi > 0$ the spectrum is monotonous for $\alpha \geq 1$. More precisely, at fixed ϕ and $N_S \gg 1$, there is a critical value of α_c, depending both on N and ϕ, such that, for $\alpha < \alpha_c$, at half-filling, all the momenta k are occupied in an alternating way, as shown in Fig.5. Thus, for $\alpha < \alpha_c$ and at half-filling, the ground-state is a BP-state, EE is linear with slope $\ln 2$ and the Fermi surface has a fractal topology with $d_{box} = 1$: this is shown in Fig.6.

For $N_S \to \infty$ one has that $\alpha_c \to 0$: this happens since, in the thermodynamic limit ($N_S = \infty$), it is not possible to define and occupy only the even momenta; however, for each N_S arbitrarily large, α_c is strictly positive. When $\alpha > \alpha_c$ only a fraction of the momenta are occupied in an alternating way, since the "zig-zag" structure of the dispersion relation is partially lost. As a result, the slope of the EE decreases, as shown in the inset of Fig.6.

B. Model B

We consider here a translational invariant chain of N_S sites with periodic boundary conditions and with eigenfunctions given by plane waves $\psi_k(J) = \frac{1}{\sqrt{N_S}}e^{ikJ}$. We assume that the Hamiltonian is such that the single-particle energy spectrum has the form

$$\varepsilon_k = -t \cdot \sin\left(\frac{1}{k^\alpha}\right), \tag{25}$$

where α is a positive odd integer. The spectrum is plotted in Fig.7 for $\alpha = 1$. The Fermi surface, in a pertinent range of fillings, has a fractal topology and, at half-filling, the Fermi energy is zero so that Fermi surface is simply given by the set of points $\{\pm\frac{1}{\pi\alpha}, \pm\frac{1}{\pi 2^\alpha} \pm \frac{1}{\pi 3^\alpha}\ldots\}$. The point $k = 0$ is an accumulation point for this set with box counting dimension [79]

$$d_{box} = \frac{\alpha}{\alpha + 1}, \tag{26}$$

so that $d_{box} = 1/2$ for $\alpha = 1$.

We numerically determined the EE for the above model (26) for increasing values of N_S as the parameter α takes the values $\alpha = 1, 3, 5$. The EE has a well defined thermodynamic limit and, for small size of the subsystem A, is well described by a power-law. In order to give a reliable estimate of this power-law growth one needs to compute the EE for $L = 1, \ldots, 128$ and fit the obtained values with the function $S_A = a + bL^\beta$ for different system sizes. One needs this procedure to get rid of finite-size effects since, even in the the short-range model, the EE shows finite-size effects when L is comparable to the system size [43]. Thus, to recover the expected logarithmic growth one has to fix L and vary N_S.

The results of this fit are reported in Fig. 8. Here we plot, on the left panel, the EE for different values of α. The results for the EE obtained for the short-range model and the BP-state are also shown for comparison. In the right panel of Fig. 8 we plot the exponent β as a function of N_S. We see that, as N_S is increased, β approaches d_{box}. Since this feature is shared also by the previous models, one is tempted to conjecture that this is a general feature of the scaling of the EE in translational invariant chains.

Our findings agree with the results presented in the Appendix of [61], where a construction of a translation invariant fermionic state violating the area law was explicitly given with Cantor-like Fermi surfaces, and with the results of [63] where, for infinitely many intervals in a spin chain, an EE of the form $S \sim L^\alpha$ was found with α possibly taking any value between 0 and 1.

We observe that in [26] a formal criterion for the growth of the EE in presence of fractal Fermi surfaces has been discussed: in particular, it was shown in that if $C_1\|h\|^{\beta_\Gamma} < \text{Vol}(\Gamma \setminus (\Gamma + h)) < C_2\|h\|^{\beta_\Gamma}$ for a small set $\|h\|$ and $0 < \beta_\Gamma \leq 1$ (with C_1 and C_2 real constants and Γ the Fermi surface), then there is a deviation from the area law with exponent $1 - \beta_\Gamma$ (see also [63, 80]). Our results imply that such coefficient β_Γ for this class of Hamiltonians is related
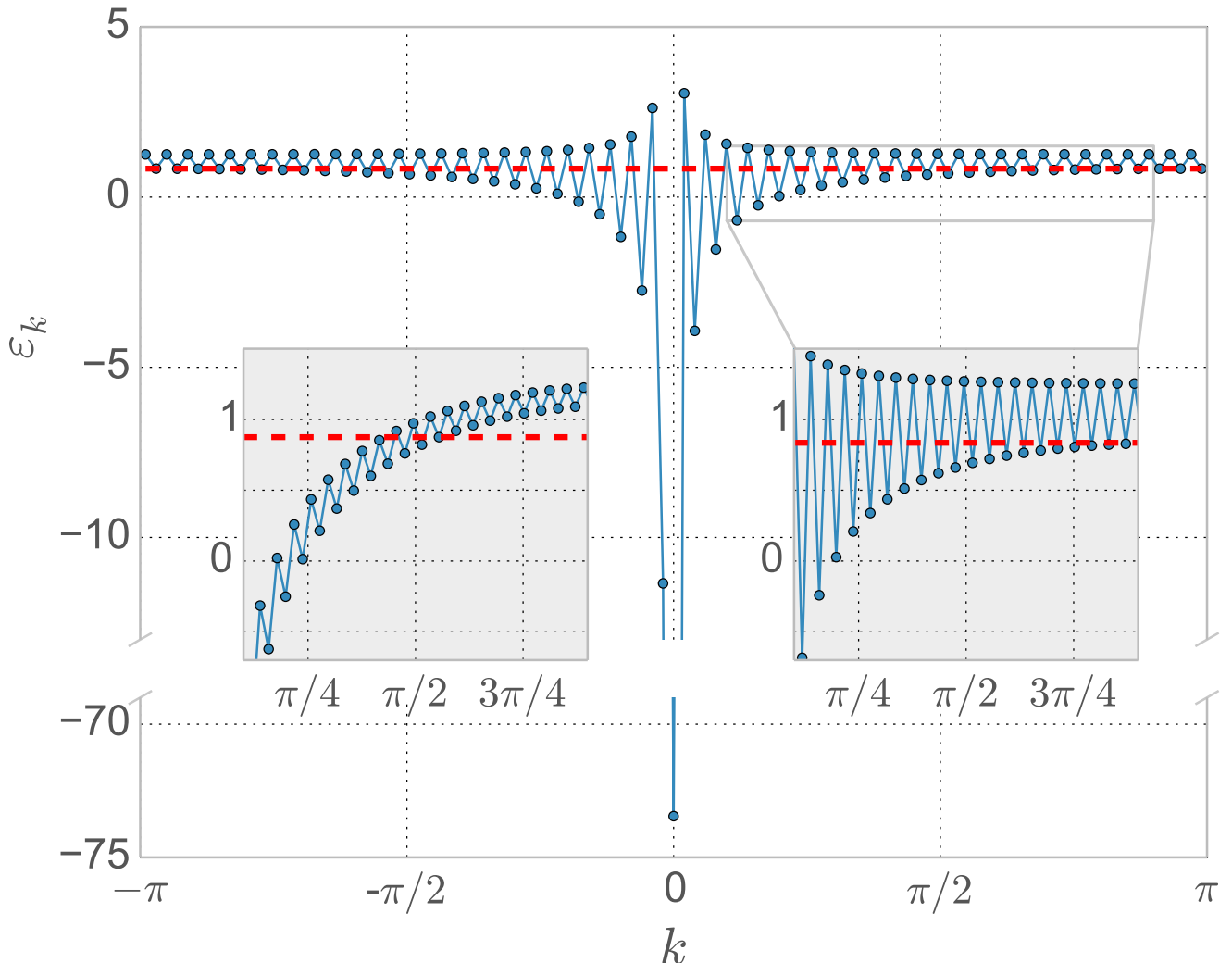
FIG. 5: Spectrum of the long-range Hamiltonian (23) with $\Phi = 0.1$, $\alpha = 0.1$, filling factor $f = 0.5$ and $N_S = 100$. Right inset: detail of the main plot showing the alternating occupation of the modes k, the Fermi energy corresponding to the dashed line. Left inset: loss of the alternating occupation increasing α, with $\Phi = 0.1$, $\alpha = 0.4$, $f = 0.5$ and $N_S = 100$.

to the box counting dimensions through $1 - \beta_\Gamma = d_{box}$: an interesting problem for future research is the study of such relation in the general case.

So far we analyzed only models in which a Fermi surface can be defined: it is natural to expect that violations of the area law may emerge also in situations where it is impossible to define a Fermi surface. When disorder is present such situation arises naturally in single realizations of disorder. In Appendix D we shall analyze a model with random long-range hoppings and we shall see how deviations from the area law may appear also in absence of the translational invariance.

V.   CONCLUDING REMARKS

We investigated how the area law for the entanglement entropy (EE) may be violated in non-interacting fermionic lattices and provided a method enabling to construct the states with maximal EE exhibiting a volume law. We called these states BP-states. For these states the EE is linear in the size of the subsystem A and the Fermi surface has fractal topology.

For translational invariant free fermionic Hamiltonians, BP-states may be obtained, at half filling, by occupying, according to Fermi statistics, even or odd momentum eigenvectors providing an explicit momentum representation of
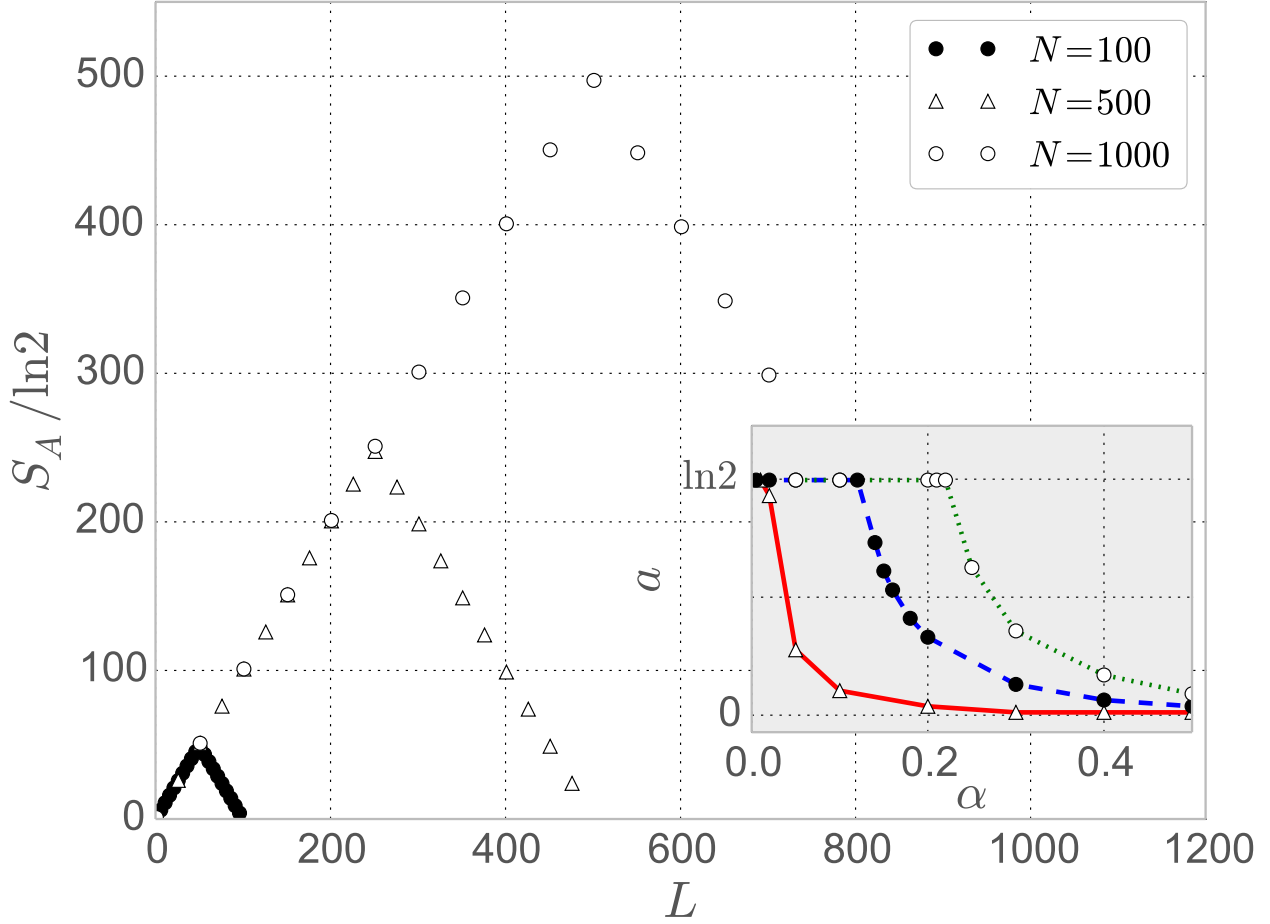
FIG. 6: Entanglement entropy as a function of the size of the block with $\alpha = 0.1$, $\Phi = 0.1$. Different total number of sites are considered: $N_S = 100$ (full circles), $N_S = 500$ (triangles), $N_S = 1000$ (empty circles). Inset: Slope of the entanglement entropy fitted with a linear function $S = aL + b$ for different values of α: $\Phi = 0.01$ (triangles), $\Phi = 0.1$ (full circles), $\Phi = 0.3$ (empty circles) and $N_S = 300$.

the state with maximal entanglement entropy. By this procedure, one originates a "zig-zag" structure of the dispersion relation leading for fermionic chains to the emergency of a fractal Fermi surface with box-counting dimension 1. By means of this procedure one can construct an explicit Hamiltonian whose ground-state supports exactly the volume law.

We then provided some examples of fermionic models for which the ground state may have an EE S_A between the area and the volume law, and we gave an explicit example of a one-dimensional free fermion model where the EE is such that $S_A(L) = a + bL^\beta$ with β being intermediate between $\beta = 0$ (area law) and $\beta = 1$ (BP-state). We saw that, also for this model, the dispersion relation has a "zig-zag" structure leading to a fractal Fermi surface whose counting box dimension equals, for large lattices, β.

It is attractive to speculate that there may be a general relation between the fractal dimension of the Fermi surface, measured by the box counting dimension, and the exponent β measuring the amount of violation of the area law for one-dimensional translational invariant free fermion lattices. Here, we only report the fact that, in all the one-dimensional examples analyzed in this paper, this relation holds true.

As a by product, our analysis shows that, a volume law for the EE cannot emerge in free fermion lattices as a result of long range hopping alone. Indeed, our analysis shows that, at least for translational invariant systems, a fractal structure of the Fermi surface is needed to establish a volume law for the EE.

Although we studied only non-interacting fermions on the lattice, our analysis is relevant also for spin models admitting a fermionic representation. Indeed, it has been recently exhibited a spin chain model supporting a volume
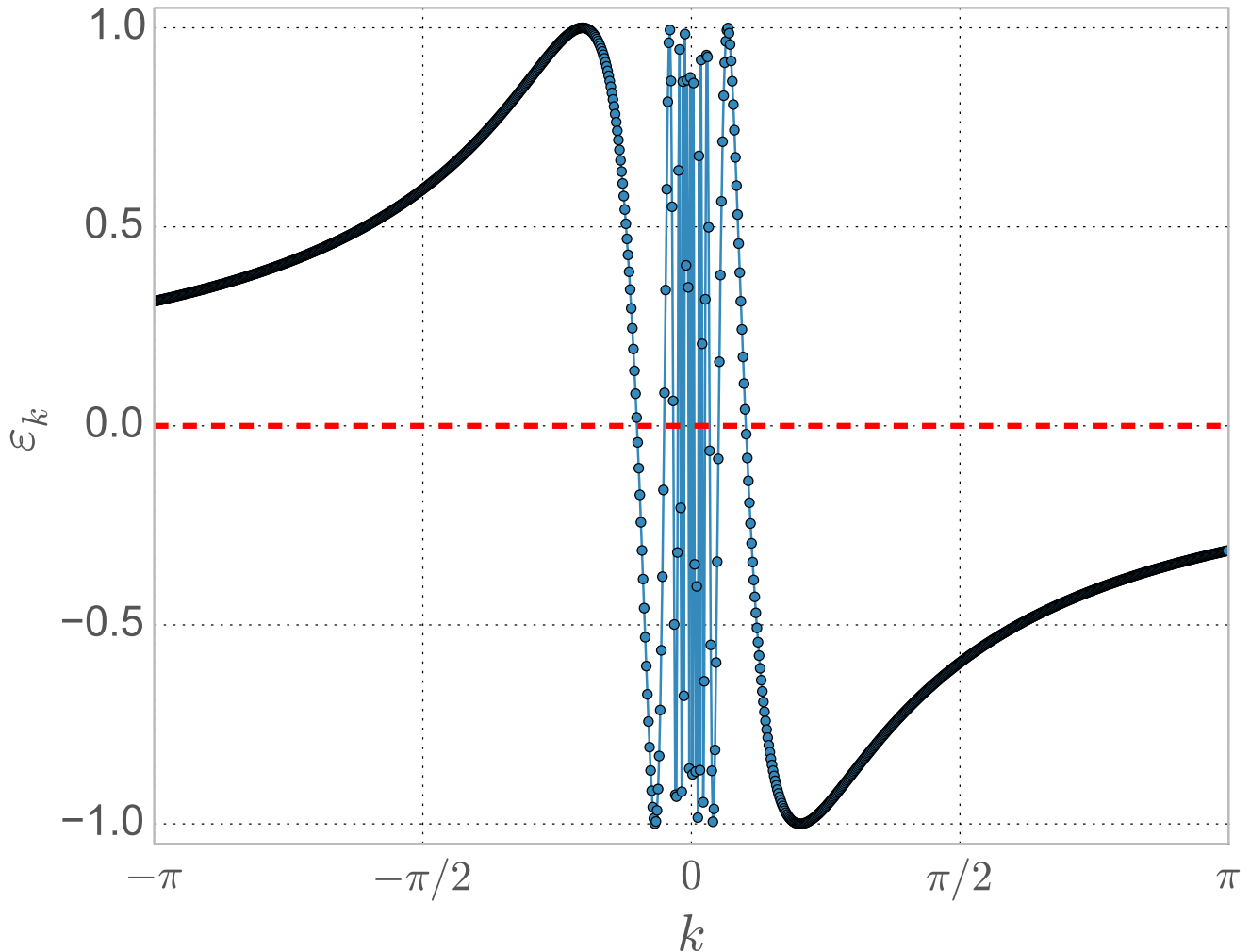
FIG. 7: Energy spectrum corresponding to (25) and $\alpha = 1$, with the thick dashed line corresponding to the Fermi energy for half-filling.

law for the EE [81]: in its fermionic representation, the Hamiltonian is highly non-local in agreement with the scenarios presented in this paper.

Note added: After the submission of this paper we noticed on the `arXiv` a very interesting paper on the power law violation of the area law in quantum spin chains [83].
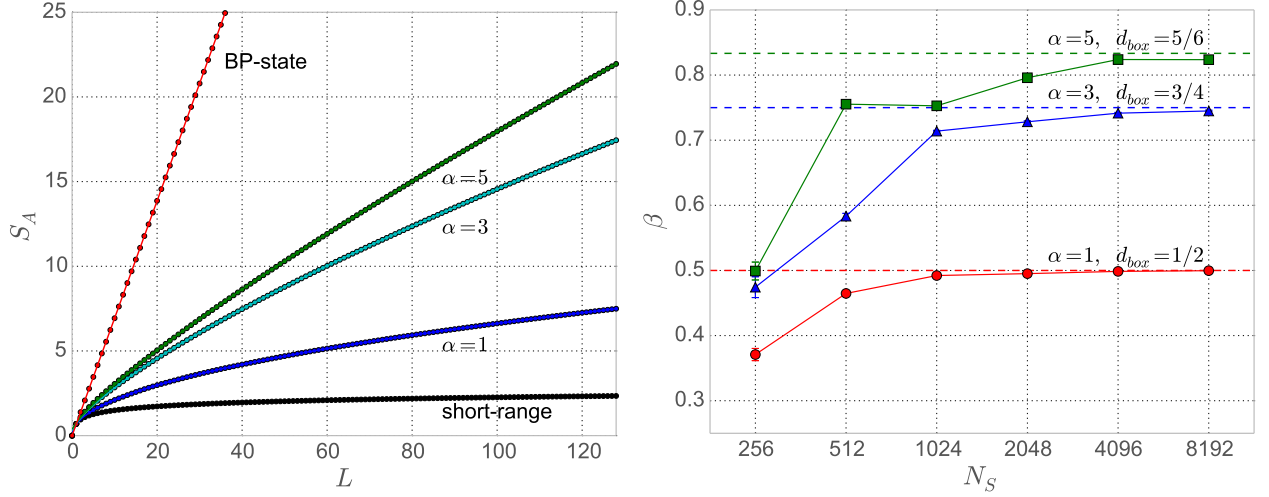
FIG. 8: Left panel: EE for the model (25) for $\alpha = 1, 3, 5$ and $N_S = 8192$. The continuous lines are the best fit lines (hardly distinguishable from the numerical points). The curves are compared with the he short-range case, exhibiting an area law, and linear behavior of a "zigzag" filling. In the short-range case the continuous curve is the best fit $S(L) = a_I + b_I \ln(L)$ where $a_I = 0.71971$ and $b_I = 0.334859$; notice how the coefficient in front of the logarithm is very close to the expected value of $1/3$. Right panel: best fit for the coefficient β (with $S(L) = a + bL^\beta$) for various system sizes and for the three values of $\alpha = 1, 3, 5$ at half-filling (circles, triangles and squares respectively). The straight lines are given by the box counting fractional dimension of the Fermi surface of the model.

Appendix A: Correlation functions and entanglement entropy

Here we derive the correlation matrix and the EE of the subsystem A for a generic graph $\mathcal{G}$ with N_S sites and N_T fermions hopping on it. The model is described by the Hamiltonian (1) and the filling is $f = N_T/N_S$ with $0 \le f \le 1$.

As in Sec. II, the sites of the lattice $\mathcal{G}$ are denoted by capital letters and the eigenvalues' equations of (1) read as

$$-\sum_{J=1}^{N_S} t_{IJ}\psi_\Gamma(J) = \epsilon_\Gamma \psi_\Gamma(I), \tag{A1}$$

where ϵ_Γ are N_S single-particle energy eigenvalues ordered so that $\epsilon_1 \le \epsilon_2 \le \cdots \le \epsilon_{N_S}$ and $\psi_\Gamma(I)$ are the corresponding N_S orthonormal eigenfunctions. Upon defining

$$d_\Gamma = \sum_{I=1}^{N_S} \psi_\Gamma(I) c_I, \tag{A2}$$

one immediately sees that the operators d_Γ obey to the canonical fermionic anticommutation relations and that the Hamiltonian (1) may be rewritten as

$$H = \sum_{\Gamma=1}^{N_S} \epsilon_\Gamma d_\Gamma^\dagger d_\Gamma, \tag{A3}$$

so that the ground-state $|\Psi\rangle$ can be written as

$$|\Psi\rangle = \prod_{\Gamma=1}^{N_T} d_\Gamma^\dagger |0\rangle. \tag{A4}$$

Given a set A, whose sites are labelled by $i, j = 1, \cdots, L$, one may define the correlation matrix C as the matrix whose entries are given by

$$C_{ij} = \langle \Psi | c_i^\dagger c_j | \Psi \rangle. \tag{A5}$$

Using (A2) and (A4), one finds

$$C_{ij} = \sum_{\Gamma=1}^{N_T} \psi_\Gamma(i)\psi_\Gamma^*(j). \tag{A6}$$

If one denotes with C_γ ($\gamma = 1, \cdots, L$) the L eigenvalues of the matrix C_{ij} one gets [27]

$$S_A = -\sum_{\gamma=1}^{L} [(1 - C_\gamma)\ln(1 - C_\gamma) + C_\gamma \ln C_\gamma]. \tag{A7}$$

Appendix B: Spectrum of model A

We analyze here the spectrum of the model, introduced in Sec. IV A. The hopping matrix reads

$$t_{I,J} = t\frac{e^{i\phi d_{I,J}}}{|I - J|_p^\alpha}, \tag{B1}$$

where

$$d_{I,J} = \begin{cases} (I - J) & if \ |I - J| \leq N_S - |I - J| \\ -N_S + |I - J| & otherwise. \end{cases} \tag{B2}$$

Due to the translational invariance, the eigenstates are plane waves, while, for finite N_S, the spectrum is given by

$$\varepsilon_k = -2t\begin{cases} \sum_{m=1}^{\frac{N-1}{2}} \frac{1}{m^\alpha}\cos((k+\phi)m) & for \ odd \ N_S \\ \sum_{m=1}^{\frac{N}{2}-1} \frac{1}{j^\alpha}\cos((k+\phi)m) + \frac{\cos(\pi n_k)}{2\left(\frac{N_S}{2}\right)^\alpha} & for \ even \ N_S, \end{cases} \tag{B3}$$

with $k = 2\pi n_k/N_S$. Even if, for finite N_S, ε_k forms a discrete set corresponding to integer values of n_k, it is most useful to provide an expression of (B3) valid for all values of k. For this purpose, Eq. (B3) may be rewritten using Lerch transcendent functions [84]:

$$\Phi(z, \alpha, a) = \sum_{j=0}^{\infty} \frac{z^j}{(j + a)^\alpha}, \tag{B4}$$

yielding

$$\varepsilon(k) = 2t\begin{cases} \Re\left[z^{\frac{N+1}{2}}\Phi(z, \alpha, \frac{N+1}{2}) - z\Phi(z, \alpha, 1)\right] & for \ odd \ N_S \\ \Re\left[z^{\frac{N}{2}}\Phi(z, \alpha, \frac{N}{2}) - z\Phi(z, \alpha, 1)\right] - \frac{\cos(\pi n_k)}{2\left(\frac{N}{2}\right)^\alpha} & for \ even \ N_S, \end{cases} \tag{B5}$$

with $z \equiv e^{i(k+\phi)}$.

Let us start by analyzing the spectrum when $\phi = 0$; this corresponds to power-law decaying hoppings. Since $\varepsilon_k = -\varepsilon_k$ one may consider only the interval of the Brillouin zone corresponding to $k = [0, \pi)$. For $\alpha \geq 1$, $\varepsilon(k)$ is a monotonically increasing function of k, so that the many-body ground-state is filled following an ascending order of $|n_k|$, just as in the short-range tight-binding model. Thus, for every value of $\alpha \geq 1$, the EE is the same of the tight binding model and, thus, follows the usual area law for the EE. For $\alpha < 1$, $\varepsilon(k)$ is an oscillating function with $\frac{N_S - (N_S \mod 2)}{2}$ maxima (and minima) almost equidistant in the interval $k = [\pi, \pi)$. In addition, the set ε_k is still monotonous in $k = [0, \pi)$ so that every wave number k lies between a different pairs of local maxima an minima. As a result, eve for $\alpha < 1$ the EE follows an area law.

If $\phi \neq 0$ the function $\varepsilon(k)$ shifts, losing its parity. For $\alpha < 1$, if one considers two consecutive ks of the discrete set ε_k one sees that the shift introduced by a small ϕ increases the energy of one of them and decreases the energy of the other. It follows that the set ε_k is no more monotone and takes a zigzag shape. As shown in Fig.5, the energies corresponding to n_k's of different parity arrange themselves on two different branches.
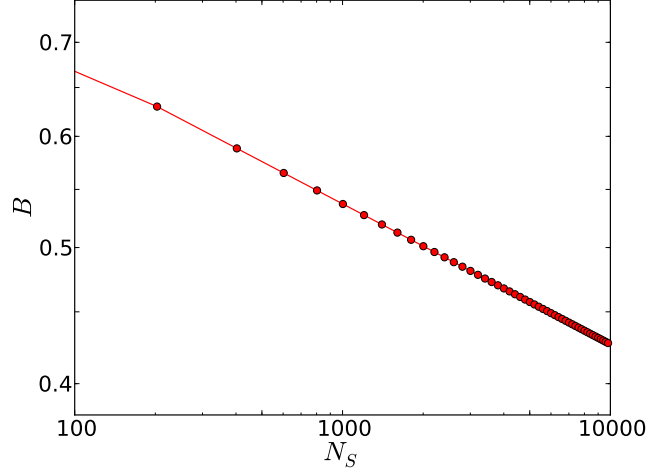
FIG. 9: Oscillation amplitude of the spectrum (B5) for $k = \pi$ and $\alpha = 0.1$.

The maximum spacing between the two branches is bounded by the amplitude of the oscillation of $\varepsilon(k)$. To give an estimate of that, one may , for $\phi = 0$, approximate $\varepsilon(k)$ around $k = \pi$ with a cosine function [84]

$$\varepsilon(k)/t \simeq A + B \cos(R(k + \delta)), \tag{B6}$$

where

$$R = \frac{N_S - (N_S \mod 2)}{2}, \tag{B7}$$

$$a = \frac{\varepsilon(\pi),}{t} \tag{B8}$$

$$b = \frac{\varepsilon'(\pi)}{t}, \tag{B9}$$

$$c = \frac{\varepsilon''(\pi)}{2t}, \tag{B10}$$

$$A = a + \frac{2c}{R^2}, \tag{B11}$$

$$B = \pm\frac{2}{R^2}\sqrt{\frac{b^2 R^2}{4} + c^2}, \tag{B12}$$

$$\delta = \frac{1}{R}\arctan\frac{bR}{2c} - \pi. \tag{B13}$$

The study of the amplitude B shows a weak polynomial dependence on the number of sites, as plotted in Fig.9, so that a zigzag behavior of the spectrum is expected for every finite N_S.

The lower branch has always negative concavity in $k = \pi$, while the top branch's concavity can be positive or negative, depending on α. In the first case and for half-filling, there appears an alternation in the occupancy of k, i.e the Fermi energy is lying between the two branches, giving rise to the BP-state described in section III. The concavity remains positive for $\alpha < \alpha_c$ and, in this regime, the EE is always maximal showing a volume law behavior with fixed slope (see inset in Fig.5). For $\alpha > \alpha_c$, as the concavity of the upper branch becomes negative, some consecutive ks close to $k = 0$ are occupied while close, to $k = \pi$ the Fermi Energy goes below the two branches. This breaks the complete alternating configuration but, for α larger but close to α_c the EE has still depends linearly on L but with a lower slope. The crossover from volume to area law occurs smoothly as α is increased.

Appendix C: The fully connected network

For $\alpha = 0$ the long-range hopping model (4) becomes simply

$$H = -\frac{t}{N_S} \sum_{I \neq J} c_I^\dagger c_J, \tag{C1}$$

where we divided the hopping coefficient t by N_S to keep the single particle spectrum lower bounded. The spectrum of (C1) is made of two eigenvalues: $\epsilon_0 = -t\,(N_S - 1)\,/N_S$ and $\epsilon_1 = t/N_S$ corresponding, respectively, to a non degenerate ground state and a $N_S - 1$ degenerate excited state. The entries $\langle c_I^\dagger c_J \rangle$ of the correlation matrix are given by

$$\left\langle c_I^\dagger c_J \right\rangle = \begin{cases} f & for & I = J \\ b & for & I \neq J, \end{cases} \tag{C2}$$

where $f = N_T/N_S$ is the filling and b has to be determined. Since the ground-state energy (more precisely, the free energy for $T \to 0$) is

$$\langle H \rangle = -t\,(N_S - 1)\,b = -\frac{t}{N_S}\,(1 - N_S) + \frac{t}{N_S}\,(N_T - 1)\,, \tag{C3}$$

it follows that

$$b = \frac{1 - f}{N_S - 1}. \tag{C4}$$

The correlation matrix has, the, the form

$$\mathbf{C} = f\mathbf{I} + b \begin{pmatrix} 0 & 1 & 1 & \\ 1 & 0 & 1 & \\ 1 & 1 & \ddots & \\ & & & 0 \end{pmatrix}, \tag{C5}$$

with eigenvalues

$$\eta_0 = (L - 1)b + f, \tag{C6}$$

$$\eta_1 = f - b. \tag{C7}$$

Inserting (C6) and (C7) into (2) one gets

$$S_A = -\,(1 - \eta_0)\ln\,(1 - \eta_0) - \eta_0 \ln\,(\eta_0) - (L - 1)\,(1 - \eta_1)\ln\,(1 - \eta_1) - (L - 1)\eta_1 \ln\,(\eta_1)\,, \tag{C8}$$

which, for $N_S \to \infty$, yields

$$S_A \approx -L\,[(1 - f)\ln\,(1 - f) + f\ln\,(f)]\,. \tag{C9}$$

From (C9) a volume law for the EE is attained. However, S_A is not a true measure of entanglement since the initial state is mixed and, in addition, the mutual information turns out to be zero. As a result, the emergence of a volume law does not lead to nonlocal correlations for this model.

In the following, we show that the mutual information is indeed zero. If A and $\bar{A}$ are two complementary sets covering the full lattice, the mutual information is defined as

$$I\,(A : \bar{A}) = S\,(A) + S\,(\bar{A}) - S\,(A \cup \bar{A}) = S_A + S_{\bar{A}} - S_T, \tag{C10}$$

where S_T is the total entropy. For a mixture of N_{deg} degenerate states, the total entropy is given by S_T

$$S_T = -\ln\frac{1}{N_{deg}}. \tag{C11}$$

Here, the degeneracy of the many-body ground state is given by

$$N_{deg} = \binom{N_S - 1}{N_T - 1}, \tag{C12}$$

so that

$$S_T = -\,[\ln\,(N_S - 1)! - \ln\,(N_T - 1)! - \ln\,(N_S - N_T)!]\,. \tag{C13}$$

In the limit of large N_S, at fixed filling, one easily obtains

$$S_T \approx N_S \left[(1 - f) \ln (1 - f) + f \ln (f)\right]. \tag{C14}$$

The entropy of the set $\bar{A}$ has an analogous expression to (C8)

$$S_{\bar{A}} = -(1 - \bar{\eta}_0) \ln (1 - \bar{\eta}_0) - \bar{\eta}_0 \ln (\bar{\eta}_0) - (N_S - L - 1)(1 - \bar{\eta}_1) \ln (1 - \bar{\eta}_1) - (N_S - L - 1)\bar{\eta}_1 \ln (\bar{\eta}_1), \tag{C15}$$

where $\bar{\eta}_0 = (N_S - L - 1)\frac{1-f}{N_S-1} + f$ and $\bar{\eta}_1 = f - \frac{1-f}{N-1}$. For large N_S (C15) becomes

$$S_{\bar{A}} \approx -(N_S - L) \left[(1 - f) \ln (1 - f) + f \ln (f)\right]. \tag{C16}$$

Finally, putting together (C8), (C15) and (C14) one gets

$$I \simeq 0. \tag{C17}$$

Appendix D: Random hopping model

Here, we present some preliminary results on a model where long-range randomness is included in the hopping matrix. EE has been studied for different disordered models [50–52, 62]; in particular, a violation of the area law has been found for free fermionic models in their metallic phase [62].

The model is defined by Hamiltonian (1) with a random long-range hopping matrix given by

$$t_{I,J} = \frac{t \cdot \eta_{I,J}}{|I - J|_p^\alpha}; \tag{D1}$$

in Eq. (D1) $\eta_{I,J}$ is a random variable assuming the values ± 1 with equal probability. This model breaks the translational symmetry; as a result, one cannot analyze the states using momentum eigenvectors. A direct diagonalization of the matrix $t_{I,J}$ is needed to compute the correlation matrix (3), whose eigenvalues are then used to compute the EE of the ground state for various sizes, L, of the subsystem A.

Our findings are summarized in Fig. 10 and are the following: for $\alpha \gg 1$, the logarithmic behavior of the random short-range model is recovered [52]. When α decreases, at fixed size N_S, the EE clearly drops off and then, at a value of α of order 1, the EE grows back again, as shown in the left part of Fig. 10. We observe that, for $\alpha \ll 1$, the EE is larger than the one of the random short-range model and it appears to be approximately linear.

To look for the asymptotic behavior of S_A, it is most convenient to allow L to vary in a fixed interval (for example between 1 and 128) and vary N_S. It turns out that, for $\alpha \lesssim 1$, a reasonable fit function has the form $S_A(L) = a + bL^\beta$. Varying N_S we plot, in the right part of Fig. 10, β as a function of N_S for three different values of $\alpha < 1$. For $\alpha \gtrsim 1$ the EE decreases as N_S increases and there is an interval of values of α where the EE becomes even smaller than the one of the clean short-range model [85]. For $\alpha < 1$, one finds a power-law behavior of S, and β appears to grow as N_S increases.

Even if not conclusive, these results seem to indicate that another way to generate a violation of the area law for the EE of the ground state is due to the effect of disorder.

[1] L. Amico, R. Fazio, A. Osterloh, and V. Vedral, Rev. Mod. Phys. **80**, 517 (2008).
[2] R. Horodecki, P. Horodecki, M. Horodecki, and K. Horodecki, Rev. Mod. Phys. **81**, 865 (2009).
[3] O. Gühne and G. Tóth, Phys. Rep. **474**, 1 (2009).
[4] U. Schollwöck, Rev. Mod. Phys. **77**, 259 (2005).
[5] R. Orús, arXiv:1407.6552
[6] A. Osterloh, L. Amico, G. Falci, and R. Fazio, Nature **416**, 608 (2002).
[7] T. J. Osborne and M. A. Nielsen, Phys. Rev. A **66**, 032110 (2002).
[8] S.-J. Gu, S.-S. Deng, Y.-Q. Li, and H.-Q. Lin, Phys. Rev. Lett. **93**, 086402 (2004).
[9] H. Li and F. D. M. Haldane, Phys. Rev. Lett. **101**, 010504 (2008).
[10] R. Thomale, A. Sterdyniak, N. Regnault, and B. A. Bernevig, Phys. Rev. Lett. **104**, 180502 (2010).
[11] R. Thomale, D. P. Arovas, and B. A. Bernevig, Phys. Rev. Lett. **105**, 116805 (2010).
[12] V. Alba, M. Haque, and A. M. Läuchli, Phys. Rev. Lett. **110**, 260403 (2013).
[13] A. Bayat, S. Bose, P. Sodano, and H. Johannesson, Phys. Rev. Lett. **109**, 066403 (2012).
[14] A. Bayat, H. Johannesson, S. Bose, and P. Sodano, Nature Commun. **5**, 3784 (2014).
[15] J. Cui, M. Gu, L. C. Kwek, M. F. Santos, H. Fan, and V. Vedral, Nature Commun. **3**, 812 (2012).
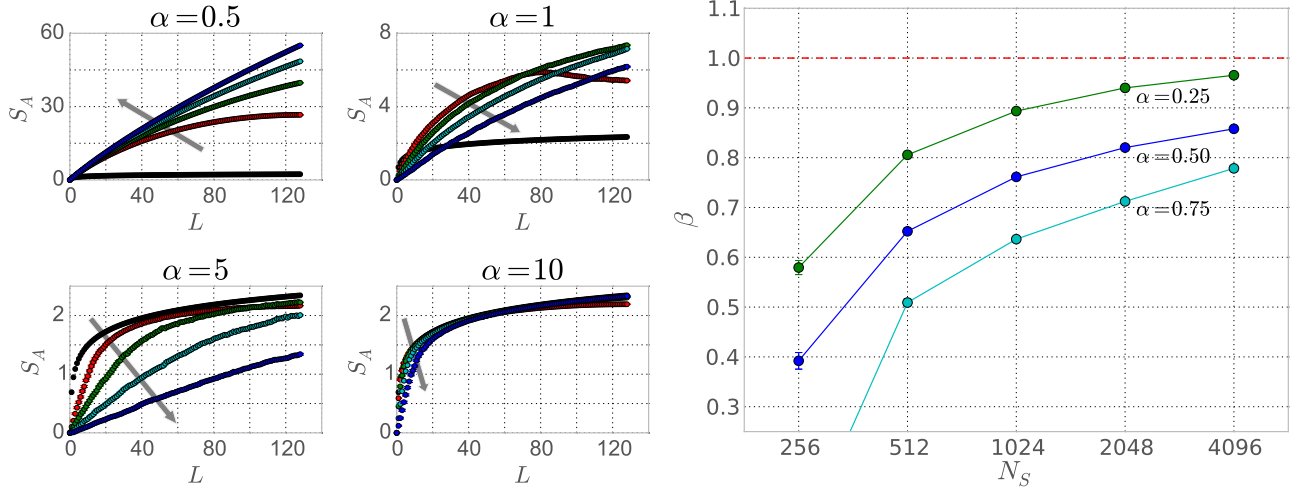
FIG. 10: Left panel: entanglement entropy calculated for four values of the decay exponent $\alpha = 0.5, 1, 5, 10$ in the random models (D1) for the sizes $N_S = 256, 512, 1024, 2048, 4096$ (and half-filling): the curves are obtained averaging over 400 realization of the disorder. The gray arrow indicates that the curves have increasing values of N_S. The curve plotted in filled black circles represent the EE for a short-range system used as a reference (note the different scales of the y-axes). Right panel: value of the fitted exponent β for three different values of α - from top to bottom $\alpha = 0.25, 0.5, 0.75$.

[16] G. De Chiara, L. Lepori, M. Lewenstein, and A. Sanpera, Phys. Rev. Lett. **109**, 237208 (2012).
[17] L. Lepori, G. De Chiara, and A. Sanpera, Phys. Rev. B **87**, 235107 (2013).
[18] F. Franchini, J. Cui, L. Amico, H. Fan, M. Gu, V. E. Korepin, L. C. Kwek, and V. Vedral, `arXiv:1306.6685`
[19] M. Srednicki, Phys. Rev. Lett. **71**, 666 (1993).
[20] J. Eisert, M. Cramer, and M. B. Plenio, Rev. Mod. Phys. **82**, 277 (2010).
[21] C. Callan and F. Wilczek, Phys. Lett. B **333**, 55 (1994).
[22] P. Calabrese and J. Cardy, J. Stat. Mech. P06002 (2004).
[23] I. Peschel, J. Phys. A **36**, L205 (2003).
[24] M. Cramer, J. Eisert, M. B. Plenio, and J. Dreissig, Phys. Rev. A **73**, 012309 (2006).
[25] M. M. Wolf, Phys. Rev. Lett. **96**, 010404 (2006).
[26] D. Gioev and I. Klich, Phys. Rev. Lett. **96**, 100503 (2006).
[27] I. Peschel, Braz. J. Phys. **42**, 267 (2012).
[28] P. Calabrese, M. Mintchev, and E. Vicari, Europhys. Lett. **97**, 20009 (2012).
[29] E. Vicari, Phys. Rev. A **85**, 062104 (2012).
[30] J. Cardy, O. A. Castro-Alvaredo, and B. Doyon, J. Stat. Phys. **130** 129 (2008).
[31] A. R. Its, B.-Q. Jin, and V. E. Korepin, J. Phys. A, **38** 2975 (2009).
[32] A. R. Its and V. E. Korepin, J. Stat. Phys **137** 1014 (2009).
[33] G. Vidal, J. I. Latorre, E. Rico, and A. Kitaev, Phys. Rev. Lett. **90**, 227902 (2003).
[34] V. E. Korepin, Phys. Rev. Lett. **92**, 096402 (2004).
[35] P. Calabrese and J. Cardy, J. Stat. Mech. P04010 (2005).
[36] P. Calabrese and J. Cardy, J. Phys. A, **42** 504005 (2009).
[37] T. Koffel, M. Lewenstein, and L. Tagliacozzo, Phys. Rev. Lett. **109**, 267203 (2012).
[38] A. Kitaev and J. Preskill, Phys. Rev. Lett. **96**, 110404 (2006).
[39] M. Levin and X. G. Wen, Phys. Rev. Lett. **96**, 110405 (2006).
[40] S. Furukawa, V. Pasquier, and J. Shiraishi, Phys Rev. Lett. **102** 170602 (2009).
[41] P. Calabrese, J. Cardy, and E. Tonni, J. Stat. Mech. P11001 (2009); *ibid.,* P01021 (2011).
[42] F. Igloi and I. Peschel, Europhys. Lett. **89**, 40001 (2010).
[43] See the Special Issue *Entanglement Entropy in Extended Quantum Systems*, eds. P. Calabrese, J. Cardy, and B. Doyon, J. Phys. A **50** (2009).
[44] B. Swingle, Phys. Rev. Lett. **105**, 050502 (2010).
[45] W. Ding, A. Seidel, and K. Yang, Phys. Rev. X **2**, 011012 (2012).
[46] T. Barthel, M.-C. Chung, and U. Schollwöck, Phys. Rev. A **74**, 022329 (2006).
[47] W. F. Li, L. Ding, R. Yu, T. Roscilde, and S. Haas, Phys. Rev. B **74**, 073103 (2006).
[48] E. A. Carlen and E. H. Lieb, `arXiv:1403.3816`
[49] I. Klich, J. Phys. A **39** L85 (2006).
[50] G. Refael and J. E. Moore, Phys. Rev. Lett. **93**, 260602 (2004); J. Phys. A **42**, 50401 (2009).
[51] I. Mondragon-Shem, M. Khan, and T. L. Hughes, Phys. Rev. Lett. **110**, 046806 (2013).

[52] G. Ramírez, J. Rodríguez-Laguna, and G. Sierra, `arXiv:1402.5015`

[53] J. Eisert and T. J. Osborne, Phys. Rev. Lett. **97**, 150404 (2006).

[54] W. Ding, N. E. Bonesteel, and K. Yang, Phys. Rev. A **77**, 052109 (2008).

[55] W. Ding and K. Yang, Phys. Rev. A **80**, 012329 (2009).

[56] N. Shiba and T. Takayanagi, `arXiv:1311.1643`

[57] G. Vitagliano, A. Riera, and J. I. Latorre, New J. Phys. **12**, 113049 (2010).

[58] H.-H. Lai, K. Yang, and N. E. Bonesteel, Phys. Rev. Lett. **111**, 210402 (2013).

[59] M. A. Metlitski and S. Sachdev, Phys. Rev. B **82**, 075127 (2010).

[60] B. Swingle, L. Huijse, and S. Sachdev, `arXiv:1309.6639`

[61] L. Huijse and B. Swingle, Phys. Rev. B **87**, 035108 (2013).

[62] M. Pouranvari and K. Yang, Phys. Rev. B **89**, 115104 (2014).

[63] M. Fannes, B. Haegeman, and M. Mosonyi, J. Math. Phys. **44**, 6005 (2003).

[64] S. Farkas and Z. Zimboras, J. Math. Phys. **46**, 123301 (2005).

[65] I. D. K. Brown, S. Stepney, A. Sudbery, and S. L. Braunstein, J. Phys. A **38**, 1119 (2005).

[66] A. Borras, A. R. Plastino, J. Batle, C. Zander, M. Casas, and A. Plastino, J. Phys. A **40**, 13407 (2007).

[67] J. E. Tapiador, J. C. Hernandez-Castro, J. A. Clark, and S. Stepney, J. Phys. A **42**, 415301 (2009).

[68] X.-W. Zha and J.-X. Qi, Int. J. Quantum Inform. **9**, 1223 (2011).

[69] X.-W. Zha, H.-Y. Song, J.-X. Qi, D. Wang, and Q. Lan, J. Phys. A **45**, 255302 (2012).

[70] W. Helwig, W. Cui, J. I. Latorre, A. Riera, and H.-K. Lo, Phys. Rev. A **86**, 052335 (2012).

[71] W. Helwig and W. Cui, `arXiv:1306.2536`

[72] W. Helwig, `arXiv:1306.2879`

[73] A. Campa, T. Dauxois, and S. Ruffo, Phys. Rep. **480**, 57 (2009).

[74] S. Hoory, N. Linial, and A. Widgerson, Bull. Amer. Math. Soc. **43**, 439 (2006).

[75] J. L. F. Barbón and J. M. Magán, JHEP **08**, 016 (2012).

[76] OEIS Foundation Inc. (2011), The On-Line Encyclopedia of Integer Sequences, `https://oeis.org/A052307`

[77] J. Riordan, *An Introduction to Combinatorial Analysis* (New York, Wiley, 1980).

[78] Indeed, considering the dimension of $\mathcal{B}$ beyond $\dim \mathcal{B} > \dim \bar{\mathcal{A}}$, proves to be detrimental for getting higher EE states. In fact if we switch $\mathcal{B}$ and $\bar{\mathcal{B}}$ due to particle-hole simmetry we see that the number of nonzero eigenvalues of C gets smaller than $\dim \mathcal{A}$.

[79] K. Falconer, *Fractal Geometry: Mathematical Foundations and Applications* (New York, Wiley, 2003) - see in particular Example 3.5.

[80] D. Gioev, `math.FA/0212215`.

[81] R. Lundgren, J. Blair, M. Greiter, A. Läuchli, G. A. Fiete, and R. Thomale, `arXiv:1404.7545`

[82] G. Ramírez, J. Rodríguez-Laguna and G. Sierra, `arXiv:1407.3456`

[83] R. Movassagh and P. W. Shor, `arXiv:1408.1657`

[84] A. Laurincikas and R. Garunkstis *The Lerch zeta-function* (Springer, 2003).

[85] Roughly, for α such that $1 \lesssim \alpha \lesssim \bar{\alpha}$, where for N_S up tp 2048 it $\bar{\alpha} \approx 10$: however, a more careful scaling analysis is required to more precisely assess and estimate $\bar{\alpha}$.